JPhys Photonics

Light source classification and colour change modelling for understanding and predicting pigments discolouration

Journal of Physics: Photonics

PAPER

Light source classification and colour change modelling for understanding and predicting pigments discolouration

Panagiotis Siozos[1,*], **Letizia Monico**[2,3,4], **Aldo Romani**[2,3], **Costanza Miliani**[5], **Brenda Doherty**[2], **Irina Crina Anca Sandu**[6], **Hartmut Kutzke**[7], **Ingrid M T Flåte**[7], **Petros Stavroulakis**[1] and **Sophia Sotiropoulou**[1,8]

[1] Institute of Electronic Structure and Laser (IESL), Foundation for Research and Technology—Hellas (FORTH), Heraklion, 71110 Crete, Greece
[2] CNR- Institute of Chemical Sciences and Technologies 'Giulio Natta' (SCITEC), via Elce di Sotto 8, 06123 Perugia, Italy
[3] SMAArt Centre of Excellence and Department of Chemistry, Biology and Biotechnology, University of Perugia, via Elce di Sotto 8, 06123 Perugia, Italy
[4] AXIS Research Group, Faculty of Science, University of Antwerp, Groenenborgerlaan 171, 2020 Antwerp, Belgium
[5] CNR-Institute of Heritage Science (ISPC), Via Cardinale Guglielmo Sanfelice 8, 80134 Napoli, Italy
[6] Munch Museum, Conservation Section, Edvard Munchs Plass, 1, 0194 Oslo, Norway
[7] Museum of Cultural History, University of Oslo, Postboks 6762 St. Olavs plass, 0130 Oslo, Norway
[8] School of Applied Arts and Sustainable Design, Hellenic Open University, Parodos Aristotelous 18, 26335 Patras, Greece
[*] Author to whom any correspondence should be addressed.

E-mail: psiozos@iesl.forth.gr

Keywords: museum lighting, colour change, pigments photodegradation, light sources, spectral composition

Supplementary material for this article is available online

OPEN ACCESS

RECEIVED
30 March 2025

REVISED
11 June 2025

ACCEPTED FOR PUBLICATION
25 June 2025

PUBLISHED
9 July 2025

Abstract

In this study, we introduce a simple but effective model, combined with a classification system for light sources based on their spectral profile approximated by the relative power distribution in the red, green and blue regions, which successfully fits experimental data of pigment colour changes in an oil binder under various lighting conditions. This model is experimentally validated by artificial ageing tests on two sets of model samples made of historical pigments (strontium yellow and Prussian blue mixed with lead white) using three white light sources (two WLEDs and a xenon light source). The model accurately fits colour shifts by analysing changes in International Commission on Illumination $L^*a^*b^*$ values. The results highlight that integrating the spectral classification of the light sources with the colour change model provides deeper insights into the causes of paint colour changes than traditional methods that rely solely on total irradiance. This combined approach enables precise prediction of long-term colour changes by exploiting the spectral characteristics of light sources.

1. Introduction

Museum lighting is a field that has evolved dynamically over the last few decades, as it has had to respond to and align with the new policies of modern museums. At the same time, it has been called upon to follow, evaluate and integrate the constantly evolving and improving products that appear on the lighting market.

Since the late 20th century, museums have consciously shifted from a traditionally inward focus on collection conservation to an outward approach centred on public engagement. This transformation has prioritised wider access to collections and a greater emphasis on interaction with the public [1]. Beyond this social dimension, museums now also face growing environmental and economic challenges. As a result, sustainability, has emerged as a third pillar—alongside access and preservation—shaping contemporary museum policies and practices [2–4].

At the same time, recent technological developments and rigorous quality testing have helped to define the requirements and formulate a quality assessment framework to achieve a balance between visibility, conservation criteria and environmental parameters [5, 6]. This framework has allowed the gradual introduction of WLED lighting systems, which for a long time were viewed with scepticism as to their

suitability for museum lighting [7]. Today, LED technology is well suited to meet the complex needs and challenges of museums and galleries, offering a practical solution when quality, energy-saving and cost-saving characteristics of these light sources are ensured [8].

In exhibition and lighting design, the selection of light sources is based on a careful balance between two primary objectives: to achieve the optimum visual presentation of artworks and cultural heritage objects, and to ensure their long-term preservation. Exposure to light, especially over time, can lead to photochemical damage, which manifests itself as colour fading, darkening, yellowing or other forms of modification due to light-induced ageing [5, 6].

This problem is not unique to museums; it has significant implications for many industries where colour is a critical component of product quality and longevity. The type, intensity and duration of light exposure play a critical role in the aesthetics, display lifetime or durability of any coloured product. Industries ranging from fashion and textiles [9–11] to packaging [12], automotive [13] and interior design face similar challenges in maintaining vibrant colours, functional properties and material integrity under varying lighting conditions.

As a result, the ability to predict and manage light-induced colour changes has become an area of extensive research. This includes artificial light-induced ageing/testing methods and predictive models to assess the impact of different light sources on colour fastness and on maintaining the visual appeal and functional performance of the product [14–17]. Advanced modelling and analysis techniques [18–21], such as spectrophotometry [22] and computational simulations [23], enable researchers and industry professionals to evaluate how specific wavelengths, spectral properties and light intensities affect colour stability. Using these methods and tools, they can predict changes in colour appearance, assess light fastness or light-induced degradation and refine lighting strategies to mitigate colour degradation, improving both the aesthetic quality and long-term durability of materials across various sectors.

Additionally, the International Commission on Illumination (CIE) has also developed lightfastness testing standards to simulate colour fading under controlled lighting conditions. CIE test methods, such as the CIE 157:2004 [24] standard and museum guidelines (e.g., ICOM, CIE), help quantify fading in colourants, assess the stability of materials under UV and visible light and provide recommendations on exposure limits.

In museum/exhibition lighting context, light source selection is typically guided by factors, such as colour rendering index and correlated colour temperature to ensure accurate and visually appealing presentation of artworks [25]. Beyond these metrics, however, the potential for light-induced damage requires careful attention.

A key challenge in assessing light exposure risk is that traditional measures, such as those based on the photopic curve (which reflects human visual sensitivity to light at different wavelengths) prioritise visual comfort and perception efficiency but do not account for the damage potential of light. Light intensity measurements in lux(lx) follow this photopic weighting, underestimating the increased damaging effects of short-wavelength, high-energy blue light (380–500 nm). As a result, even low-intensity LED lighting can cause unintended harm through photochemical reactions in materials that absorb strongly in the blue region of the spectrum. While LED lighting is energy efficient and flexible in design, it often contains a significant blue light component. Blue light photons are relatively high in energy, and when absorbed by sensitive compounds, particularly those found in yellow and some red pigments, they can initiate photochemical processes. Importantly, photochemical damage depends not only on photon energy but also on how strongly a material absorbs that wavelength. Therefore, to mitigate this hidden risk, museum lighting assessments must go beyond traditional metrics and consider the full spectral profile of the light source, with particular attention to high-energy blue wavelengths and the specific absorption characteristics of the materials being illuminated.

In this work, we propose a simple yet effective model, integrated with a classification system for light sources based on their spectral power distribution components (blue, green, red). The model accurately represents experimental data on pigment colour changes in an oil binder under various lighting conditions and has been validated through artificial ageing tests on light-sensitive pigments commonly used by 18th and 19th century painters—strontium yellow and Prussian blue mixed with lead white—using three light sources (two WLEDs and one xenon lamp).

However, the model does not account for other potential causes of colour change, particularly those resulting from the formation of secondary degradation products, pigment—binder interactions, or environmental factors that may amplify light-induced changes. Over time, chemical transformations within pigments can generate degradation products that alter their optical properties and perceived colour. In addition, pigment-binder interactions can impact dispersion, surface chemistry, or photochemical stability, further affecting colour stability. Environmental factors such as humidity, temperature fluctuations and

exposure to pollutants can accelerate pigment degradation, as evidenced by chromatic shifts, due to oxidation, hydrolysis, or other physicochemical mechanisms.

Despite these limitations, our findings demonstrate that combining spectral classification with the colour change model provides deeper insights into the causes of pigment colour changes than traditional approaches. This integrated method improves the accuracy of long-term colour change predictions by exploiting the spectral characteristics of light sources. In addition, its simplicity ensures accessibility to both conservation specialists and non-specialists, making it a practical tool for monitoring and preserving artworks.

2. Materials and methods

2.1. Oil paint mock-ups

A series of linseed oil paint mock-ups (figure 1) were prepared using the following commercial pigments: (i) strontium yellow (i.e., strontium chromate; Alfa-Aesar); and (ii) Prussian blue (Kremer Pigmente) mixed with lead white (hydrocerussite, Sigma-Aldrich) in a weight ratio of approximately 1:50. The pigments were chosen for their varying levels of photochemical reactivity within the oil binder, as reported in previous studies [26–35]. Oil-to-pigment mixtures (weight ratio ≈1:4) were applied onto a polycarbonate substrate to create paint films with an average thickness of approximately 200 μm. The samples were then left to dry in the dark for about two months. Additionally, a series of control samples consisting of pure raw linseed oil (Zecchi, Florence) were also prepared [36].

2.2. Accelerated ageing experiments and experimental monitoring of colour changes

To ensure a reliable evaluation of the method proposed in this study, it is essential to thoroughly characterize the illumination sources used. This requires documenting several key parameters, including the spectral distribution of the light source, the type of filter used to modulate its spectral emission, and the average irradiance (measured in W cm^{-2}) at the sample's position. Additionally, the average temperature (in °C or K) and relative humidity at the sample's position were recorded, alongside the colour temperature of the light source and the total exposure time (in hours).

2.2.1. Light sources and spectroradiometric measurements

Photoageing experiments of oil paint mock-ups were performed using the following set-ups: (i) a Cermax xenon lamp filtered in the UVB, UVC and IR regions (irradiance: 0.030 ± 0.01 W cm^{-2}; total radiant exposure: 0.21 ± 0.01 Wh cm^{-2}); (ii) two white WLEDs lights with colour temperature at 4000 K and 2700 K (irradiance: ≈0.019–0.020 W cm^{-2}; total radiant exposure: ≈ 0.177–0.194 Wh cm^{-2}), selected via a tunable WLEDs prototype developed by F&M Progetti srl (Prato, Italy). These devices were chosen to represent varying emissions in the violet-blue region of visible light and to reflect the widespread use of 4000 K and 2700 K WLED systems in modern museum lighting. Temperature ($T \approx 30$ °C–35 °C) and relative humidity (RH% ≈ 30%–40%) were regularly monitored during the experiments using a thermo-hygrometer [6].

An irradiance-calibrated AvaSpec-2048-2 spectrometer (Avantes, NL) equipped with a 200 mm diameter optical fibre (FC-UVIR200-2 ME, Avantes) and an 8 mm active area cosine corrector (CC-UV-VIS/NIR, Avantes) was used to record the emission spectra of the white light sources used in the ageing experiments (figure 2). The spectrometer operates in the 171–1100 nm range, employing a 300 lines mm^{-1} grating. It is equipped with an AvaBench-75 optical bench; with a 25 mm slit, this configuration yielded a 1.2 nm FWHM spectral resolution. A 2048-pixel CCD detector is used for detection. Measurements were performed at the sample position using an integration time of 5–80 ms and 5–10 accumulations. The source profiles (figure 2) and corresponding irradiance values were obtained by averaging 10–20 spectral data collected throughout the experiment. Irradiance was measured in the 350–1100 nm for ageing experiments conducted with the xenon source, and over the 300–830 nm range for those conducted with the two WLEDs lamps.

Information about the radiant exposure protocol, including the duration of the photoageing experiments, irradiance, and total radiant exposure for each light source, is provided in table 1. In addition, plots of L^*, a^*, and b^* values as a function of illumination time for both paints under all three light sources used in this study are presented in the supplementary material. The experiments conducted reached a maximum radiant exposure ranging from 0.17 to 0.21 Wh cm^{-2}, depending the light source. These values were selected because the rate of change in the CIE $L^*a^*b^*$ coordinates at this level approaches a plateau, enabling a more stable and reliable analysis of the ageing effect.

Finally, the photoaging apparatus was designed to minimize temperature increases on the surface of the samples, using light sources with limited heat output and ensuring sufficient ventilation. The xenon lamp was filtered in the UVB, UVC, and IR regions, while the selected LED light sources had emission spectra confined to the visible range, with no ultraviolet or infrared output. As a result, they did not introduce any

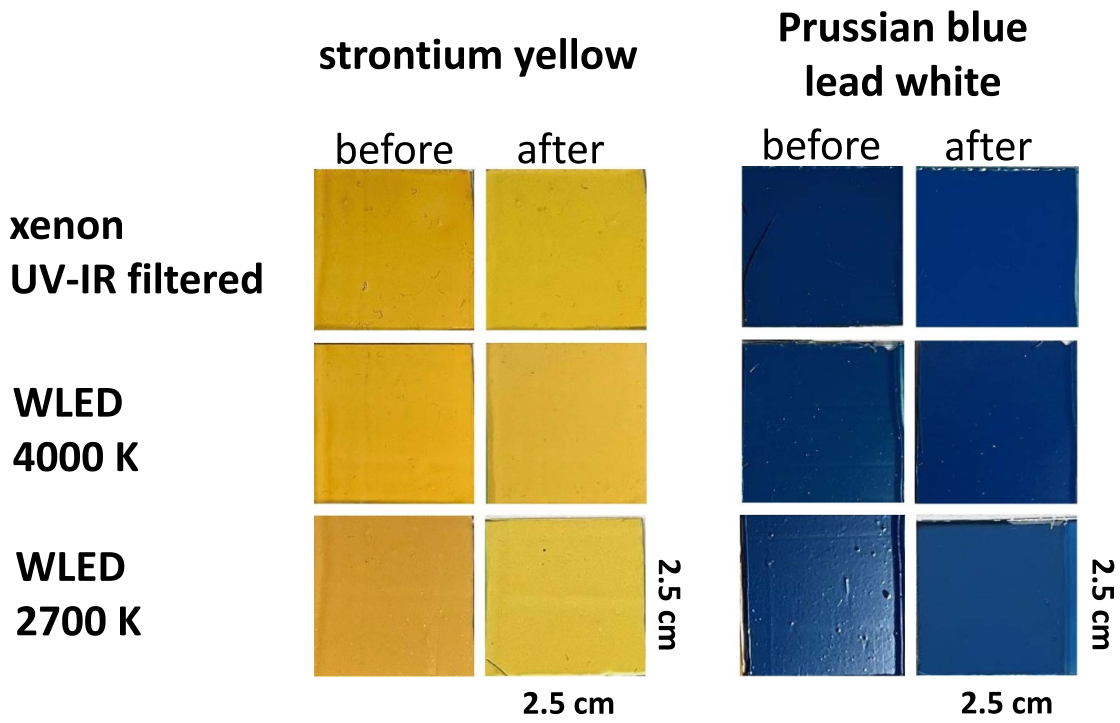

Figure 1. Images of strontium yellow and Prussian blue-lead white oil paints before and after artificial ageing using the three white light sources.

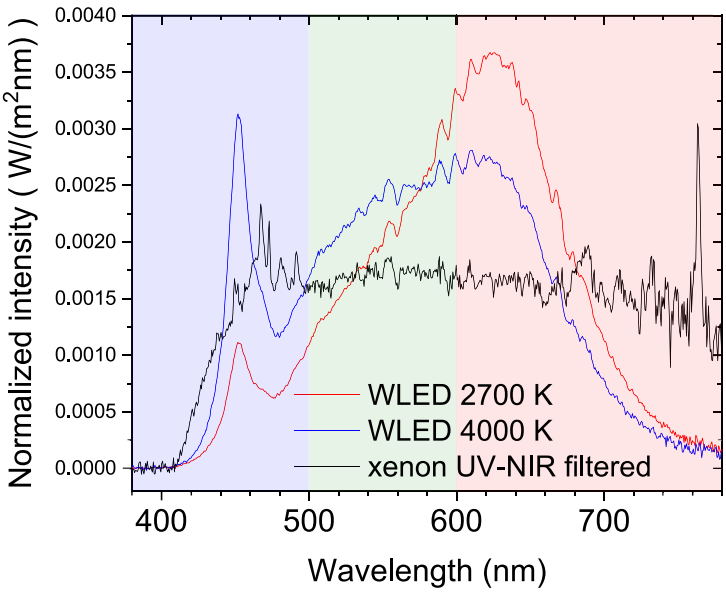

Figure 2. Diagram of the spectral ranges selected for light source classification. Blue, green and red area corresponds to 380–500, 500–600 and 600–780 nm respectively.

significant thermal effect on the surface of the specimens. This setup reflects typical museum lighting conditions, which do not generally result in substantial heating of artworks. Therefore, thermal effects were considered negligible under the tested conditions. However, temperature may play a more significant role in pigment degradation in applications involving high-intensity lighting or outdoor exposure, and should therefore be taken into account in future studies.

2.2.2. VIS diffuse reflectance spectroscopy and colorimetry

Colorimetry was carried out by Konica-Minolta CM700D furnished with a pulsed xenon lamp emitting in the visible spectral range, an integrating sphere with a 40 mm internal diameter and a silicon photodiode array detector. A D65 standard illuminant and 2° angle observer were used for the conversion of the spectra

Table 1. RGB spectral values, exposure duration, irradiance, and maximum radiant exposure of the photoageing experiments for each light source.

Light source	V_B 380–500 nm	V_G 500–600 nm	V_R 600–780 nm	Ageing Duration min	Irradiance mW cm^{-2}	Max Radiant Exposure Wh cm^{-2}
WLED2700 (warm LED)	9	36	55	600	19.4	0.194
WLED4000 (cold LED)	20	41	39	540	19.7	0.177
Xenon	20	30	50	420	30.0	0.210

Table 2. Spectral ranges selected for the calculation of a light source percentage of power distribution.

Classification	Spectral range (nm)	
	Low	High
Red spectral range (R)	380	500
Green spectral range (G)	500	600
Blue spectral range (B)	600	780

(recorded in the 360–740 nm range and with 10 nm spectral resolution) into CIE $L^*a^*b^*$ chromatic coordinates (specular reflection excluded). After a black and white calibration of the instrument with a specific standard (Spectralon), measurements were recorded before, during and at the end of the photoageing experiments. The time interval acquisition was selected depending on the measured irradiance at the sample position. For a defined light source, accelerated lightfastness experiments were performed by keeping comparable total radiant exposure values.

2.3. Light source classification based on their spectral power distribution

We propose a straightforward, simplified approach for classifying light sources based on their spectral characteristics. This method is designed to be accessible to users without specialist knowledge. The classification model categorizes light sources based on their power distribution across spectral ranges corresponding to the primary colours of light, as perceived by the human eye within the visible spectrum (figure 2). This approach aligns with museum lighting practices, where emissions outside the visible spectrum are typically filtered out. As a result, light sources are classified using only three numbers, representing the percentage of power distribution across different visible spectral ranges (table 2).

Therefore, for each light source the V_R, V_G and V_B correspond to the percentage of emission in the specific (R, G, and B) spectral range over the emission in the entire spectral range of the source from 380 to 780 nm. Thus:

$$V_R = \frac{\text{Red spectral range}}{\text{Total emission in visible}} 100\% \tag{1}$$

$$V_G = \frac{\text{Green spectral range}}{\text{Total emission in visible}} 100\% \tag{2}$$

$$V_B = \frac{\text{Blue spectral range}}{\text{Total emission in visible}} 100\%. \tag{3}$$

This approach assumes that light-induced colour change in a material is primarily driven by irradiance within a specific spectral region (V_B, V_G, or V_R), rather than by the total irradiance across the entire spectrum. In other words, if a pigment is exposed to light within the spectral range to which it is most sensitive, the resulting colour change will be comparable to that observed under full-spectrum illumination, as long as the amount of the effective irradiance component remains the same. This is because photodegradation is caused by the portion of the spectrum that the pigment absorbs.

For varied materials, an experimental study using mock-up samples is necessary to validate this assumption and identify the specific spectral component responsible for damage in each pigment. Finally, the V_B, V_G, or V_R values of the light sources used in this study are presented in table 1.

Although the RGB-based classification is a practical and accessible method of categorising light sources spectrally, it inevitably oversimplifies the complexity of the illumination spectra. In our study, however, this approach is valid and acceptable given the spectral characteristics of modern museum lighting sources, which are typically continuous and limited to the visible range either by design or through the use of filters that exclude UV and NIR radiation. Additionally, the pigments considered here generally exhibit broad

absorption and reflectance features in the visible range, making them less susceptible to variations in illumination across narrow spectral bands.

However, this simplification may limit the model's applicability in scenarios involving light sources with sharp spectral features or broader spectral content, such as natural sunlight or specialized industrial lighting. In such cases, a more detailed spectral breakdown or the use of continuous spectral weighting functions may be necessary to enhance prediction accuracy.

2.4. Colour change model

The model presented in this study assumes that any change in the colour of a material, measured as a shift in the L^*, a^*, b^* values (which correspond to changes in the visible diffuse reflectance spectra), is primarily caused by photochemical reactions affecting the pigment. These reactions alter the pigment's chemical composition, leading to a reduction in the concentration of its original state. The model correlates colour changes with this reduction in pigment concentration. However, other factors, such as loss of gloss or yellowing of the binding medium, can also contribute to colour shifts and influence the measured colorimetric values. While these effects are not included in the model, they should be considered when interpreting the results.

When exposed to light, the material absorbs radiation, initiating photochemical reactions that reduce the pigment's concentration. At low light absorption rates (zero-order reaction), the rate of this reduction is proportional to the absorbed light energy and can be expressed by the equation:

$$\frac{\mathrm{d}n}{\mathrm{d}E} = -\Phi \text{ or } n = n_0 - \Phi E \tag{4}$$

where n is the concentration of the pigment after irradiation with energy E, n_0 is the initial concentration of the pigment in the material and Φ is the quantum yield of the reaction. However, variations in the concertation of the pigments will result in a change in the percentage of the irradiation that interacts with the pigment molecules. This can be expressed by the equation:

$$\frac{dE}{dn} = -AE \text{ or } E = E_0\, e^{-An} \tag{5}$$

where E is the energy absorbed by the pigment, E_0 is the total energy that has been irradiated, and A is a constant related to the penetration depth of the light and the absorption/scattering cross section [37]. Based on these and equations (4) and (5) we can derive that:

$$n = n_0 - \Phi E_0\, e^{-An},\ n_0 - n = \Phi E_0\, e^{-An}. \tag{6}$$

Photochemical reactions in pigments are generally slow processes, resulting in only minor changes in pigment concentration during irradiation. Based on this observation, we define the parameter:

$$\varepsilon = \frac{n_0 - n}{n_0} \tag{7}$$

where $\Delta n = n - n_0$ is the change in pigment concentration over time, n_0 is the initial concentration of the pigment. The 'small perturbation parameter' ε is a dimensionless quantity that represents the relative change in pigment concentration due to photodegradation. The assumption $|\varepsilon| \ll 1$ implies that this change is small, which is valid for slow degradation processes where pigment concentration varies minimally over the exposure period. In modelling, ε facilitates the linearization of complex equations or the application of asymptotic (e.g., exponential) expansions. It also serves as a metric for assessing the sensitivity of colour or reflectance changes to minor pigment losses. This approach enables small but perceptible ΔE shifts in the CIE $L^*a^*b^*$ space to be interpreted in terms of ε. By mapping reflectance or colour measurements over time onto ε values, even subtle colour changes due to pigment degradation can be monitored. Under these conditions, ε remains approximately constant, allowing for the linearization of the exponential decay described in equation (6). Under this approximation, equation (6) can be expressed as:

$$\varepsilon = \frac{\Phi E_0}{n_0} e^{-An}. \tag{8}$$

Rearranging equation (8), we subsequently obtain an explicit relationship for n:

$$n = -\frac{1}{A} \ln\left(\frac{\varepsilon n_0}{\Phi E_0}\right) = -\frac{1}{A} \ln\left(\frac{\varepsilon n_0}{\Phi}\right) + \frac{1}{A} \ln\left(E_0\right). \tag{9}$$

Any colorimetric changes (C_c) expressed either in the $L^*a^*b^*$ colour space, or in $\Delta E1976$ or in diffuse reflectance spectral changes are assumed to be proportional to the concentration n of the pigment in the paint [38]. Thus, equation (9) can be rewritten in terms of colorimetric changes as:

$$C_c = -\frac{1}{A'}\ln\left(\frac{\varepsilon n_0}{\Phi E_0}\right) = -\frac{1}{A'}\ln\left(\frac{\varepsilon n_0}{\Phi}\right) + \frac{1}{A'}\ln(E_0)\,. \tag{10}$$

Equation (10), presenting a linear relationship between colorimetric changes and $\ln(E_0)$, can be used as a practical tool for validating the proposed model and predicting colour changes.

In this formulation, the quantum yield Φ represents the efficiency of the photochemical process, defined as the number of molecules degraded per photon absorbed. While in principle Φ could be experimentally determined via chemical or spectroscopic analysis, in the current model it is used as a proportionality factor included within the slope of the linear fit between colour change and the logarithm of radiant exposure (see equation (10). As such, both Φ and ε are not measured directly, but are embedded in the empirical validation of the model, serving to support its applicability to light-induced colour change data derived from mock-up experiments.

The model, as currently formulated, is optimized for single pigments or binary mixtures in which one pigment (exerts a dominant influence on the resulting colour) predominantly determines the chromatic outcome. Extending its application to more complex composite systems, such as multi-pigment mixtures, would require accounting for the distinct spectral sensitivities and degradation kinetics and potential interactions among the pigments. This includes modelling how each pigment contributes to the overall reflectance and how the individual photodegradation rates may influence the system's optical evolution over time (how their degradation pathways evolve concurrently or competitively). Similarly, the model assumes a constant oil-to-pigment ratio and attributes colour changes predominantly to pigment degradation. In practice, experimental systems with variable binder-to-pigment ratios would allow for the investigation of colour changes resulting from the interplay of optical properties (such as surface gloss or matting effects, scattering/absorption properties, translucency/haze), where binder degradation may have a more pronounced impact than pigment alteration alone.

Addressing these limitations will require future modelling strategies that account for both additive and interactive pigment responses, as well as matrix effects introduced by varying pigment-to-binder ratios. In this context, machine learning and statistical approaches offer promising tools for capturing nonlinear relationships and complex interactions, potentially enabling more accurate and generalisable predictions across a broader range of material compositions and application scenarios [39, 40].

3. Results and discussion

Figure 3 shows the VIS reflectance spectra recorded from strontium yellow and Prussian blue mixed with lead white paints at different stages of photoageing under various white light sources. In the strontium yellow paints, irradiation induces the most pronounced spectral changes in the 500–600 nm range, with the gradual emergence of a band around 560 nm. For Prussian blue–lead white paints, a gradual increase in reflectance is observed between 460 and 470 nm under irradiation. These spectral changes, quantified by calculating the L^*, a^*, and b^* coordinates, follow a consistent trend across all three white light sources during photoageing.

Figures 4(a)–(c) illustrate the relationship between the L^*, a^*, and b^* values and the total radiant exposure of strontium yellow paint. Notably, the a^* values exhibit consistent changes regardless of the light source used for artificial ageing. In contrast, the L^* values vary depending on the light source, while the b^* values remain relatively constant, showing almost no change across different light sources or levels of total radiant exposure.

Light-induced colour change in the paint is determined not by the total irradiance over the entire emission spectrum, but by the irradiance in a specific spectral region that corresponds to the part of the spectrum that the pigment absorbs, i.e. the spectral region that is most sensitive. In this context, it is not necessary to consider in the calculations the total irradiance that illuminates the material. Instead, only the fraction corresponding to the spectral component that affects the pigment should be considered. To determine the spectral component affecting the pigment, we plotted the values of L^*, a^* and b^* as a function of each of the spectral components R, G, B of the radiant exposure for each light source. The three spectral components of radiant exposure were calculated using the following equations:

$$H_{\mathrm{B}} = \frac{V_{\mathrm{B}}}{100} H_{\mathrm{Total}} \tag{11}$$

$$H_{\mathrm{G}} = \frac{V_{\mathrm{G}}}{100} H_{\mathrm{Total}} \tag{12}$$

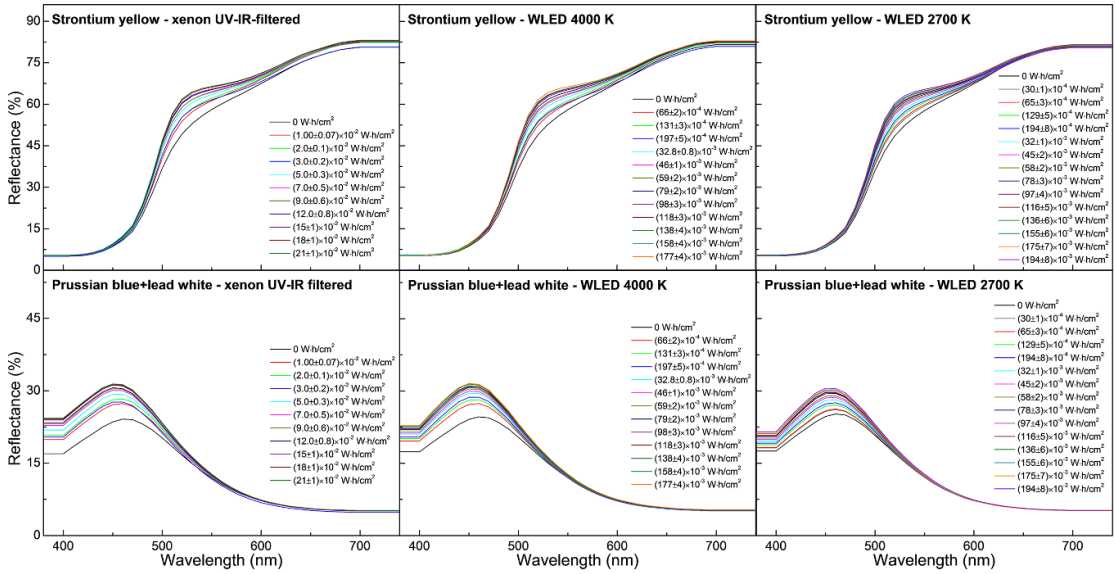

Figure 3. VIS reflectance spectra recorded from strontium yellow (top) and Prussian blue with lead white paints at different photoageing stages using various white light sources.

$$H_R = \frac{V_R}{100} H_{\text{Total}} \tag{13}$$

where H_{total} is the total radiant exposure, V_{B}, V_{G} and V_{R} the percentage of emission in the specific spectral range derived from equations (1)−(3) and H_{B}, H_{G} and H_{R} the blue, green and red radiant exposure respectively.

The results are presented in figures 4(a)–(m). We observed that for strontium yellow, the plot of L^* values versus the blue component of radiant exposure (figure 4(d)) showed significantly smaller variations between different light sources compared to the corresponding plot on total radiant exposure. This observation suggests that for the strontium yellow in the oil binder, the lightness (L^* value) of the colour is primarily affected by the light source emission in the blue range (380–500 nm). The same amount of radiant exposure in the blue region has the same effect on the examined pigment, regardless of the different total spectral power distribution of the light source. In contrast, the a^* and b^* values exhibited higher correlation with the total radiant exposure than any of the individual spectral components of radiant exposure (380–500 nm, 500–600 nm or 600–700 nm). These observations suggest that the proposed light source classification method can help in the spectral determination of harmful radiation for specific photosensitive pigments in order to selectively limit/avoid it by choosing an alternative source in the lighting design process. We performed a similar analysis for the oil paint mock-ups consisting of Prussian blue mixed with lead white. The L^*, a^*, and b^* values were plotted against the total radiant exposure (figures 5(a)–(c)) and it was found that the colour changes depended on the light source. As for strontium yellow, we plotted these values against the blue, green and red radiant exposure, based on the spectral features of the light sources. In addition to the finding that the gradual changes in CIE $L^*a^*b^*$ values due to overexposure depend on the light source, it was also observed that the a^* and b^* values show less variation across different light sources when plotted against the blue spectral component of the radiation. This suggests that the blue spectral emission plays a critical role in light-induced colour changes in pigments, as predicted by this model. These consistent observations further support the initial hypothesis behind the proposed method. By applying a simple tri-spectral categorization of light sources, this method provides an efficient way to model expected light-induced colour changes based on their spectral characteristics.

To quantify these observations, we applied the colour-change model described in this study to develop effective models for colour prediction. Using equation (10), we calculated the natural logarithm of the total radiant exposure and the radiant exposure of the individual spectral components. All L^*, a^*, and b^* values from all light sources were plotted against the natural logarithm of the radiant exposure for strontium yellow (figure 7) and Prussian blue-lead white paint mock-ups (figure 7). In all cases, the L^*, a^*, and b^* values exhibited a strong linear relationship with radiant exposure when plotted on a logarithmic scale, demonstrating the validity of the proposed colour change model. This correlation suggests that the rate of colour change follows a predictable trend.

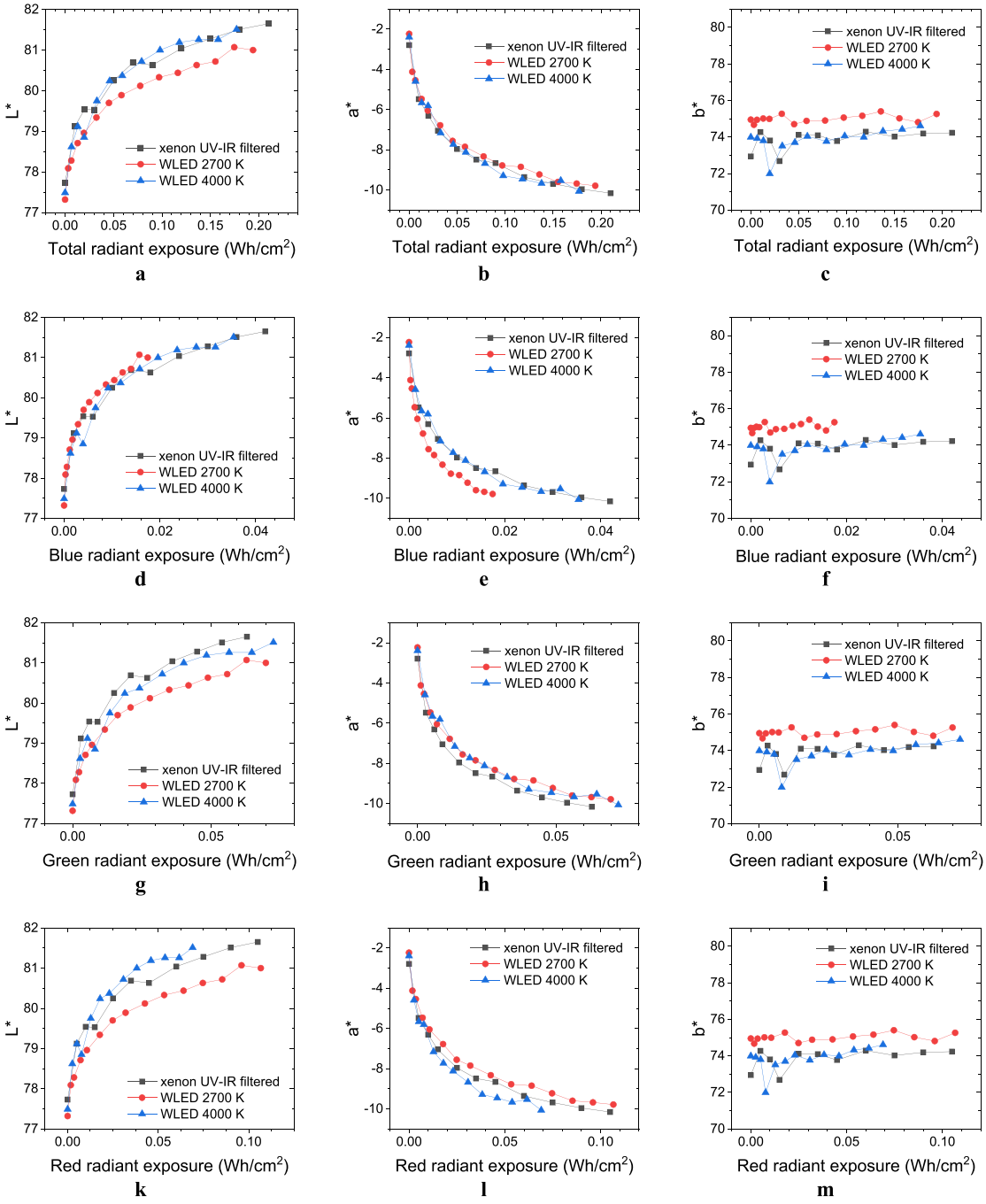

Figure 4. Plots of L^*, a^*, and b^* values as a function of radiant exposure for strontium yellow oil paints. The four rows correspond to total, red, green, and blue spectral components of the radiant exposure, respectively. Each column represents one of the CIE $L^*a^*b^*$ coordinates (L^*, a^*, b^*). The influence of each spectral component on colour changes can be assessed by comparing the plots across the columns.

For strontium yellow, we obtained an R^2 value of 0.92 when plotting L^* values against the total radiant exposure (figure 6(a)). This value increased slightly to 0.95 but clearly when using the blue component of the radiant exposure (figure 6(c)). Conversely, the a^* values showed a higher R^2 value (0.98) for the total radiant exposure than for any individual spectral component (figures 6(b) and (d)).

For Prussian blue-lead white, the data points were more dispersed compared to strontium yellow, resulting in lower R^2 values. In the plot of L^* values, we observed a slight improvement in R^2 when using the red component of the radiant exposure compared to the total radiant exposure (figures 7(a) and (d)). A significantly higher R^2 value (0.84) was found for the a^* values when using the blue component compared to the total radiant exposure ($R^2 = 0.60$). Similarly, for the b^* values, we observed an improved R^2 (0.89) when using the blue component compared to the total radiant exposure ($R^2 = 0.71$). This further emphasizes the

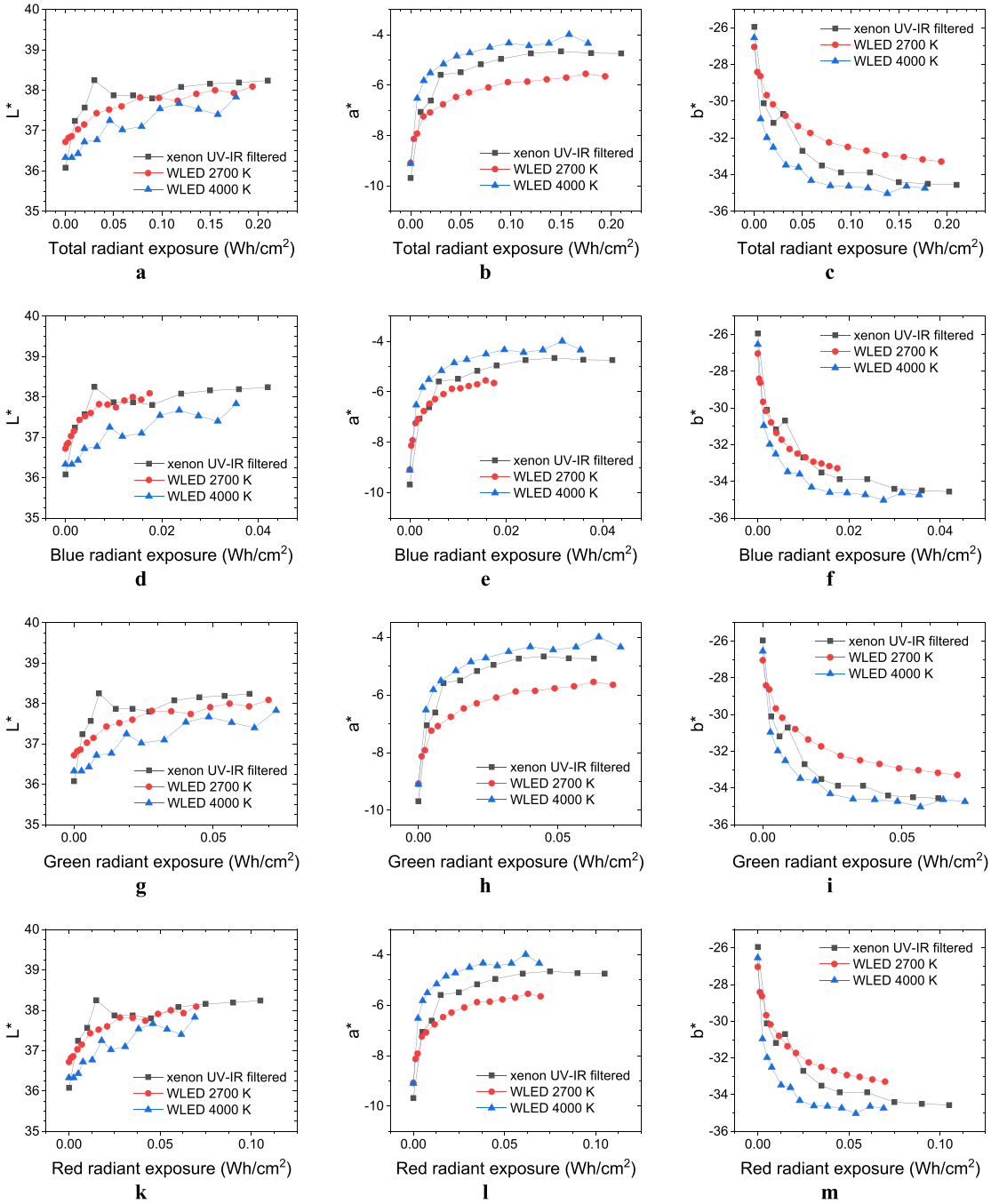

Figure 5. Plots of L^*, a^*, and b^* values as a function of radiant exposure for Prussian Blue-lead white oil paints. The four rows correspond to total, red, green, and blue spectral components of the radiant exposure, respectively. Each column represents one of the CIE $L^*a^*b^*$ coordinates (L^*, a^*, b^*). The influence of each spectral component on colour changes can be assessed by comparing the plots across the columns.

dominant influence of the blue component in the colour change of Prussian blue, aligning with previous studies on the wavelength-specific fading behaviour of the pigment [41].

The strong linear relationships observed in figures 6 and 7 validate the colour-change model and confirm that blue spectral emission plays a critical role in the light-induced colour changes in pigments. These findings clearly support the assumption that the light-induced colour change depends on the spectral composition of the light source's emission. Therefore, it is advisable to consider not only the total radiant exposure but also its spectral distribution, even as a rough approximation, such as the percentage of the spectrum in the blue, green and red range. This confirms that the integration of the proposed light source classification system with the colour-change model built for a specific pigment-binder system provides a robust and practical method for predicting pigment degradation. By separately accounting for the influence of individual spectral bands of radiation, this approach offers a more precise and accessible tool for

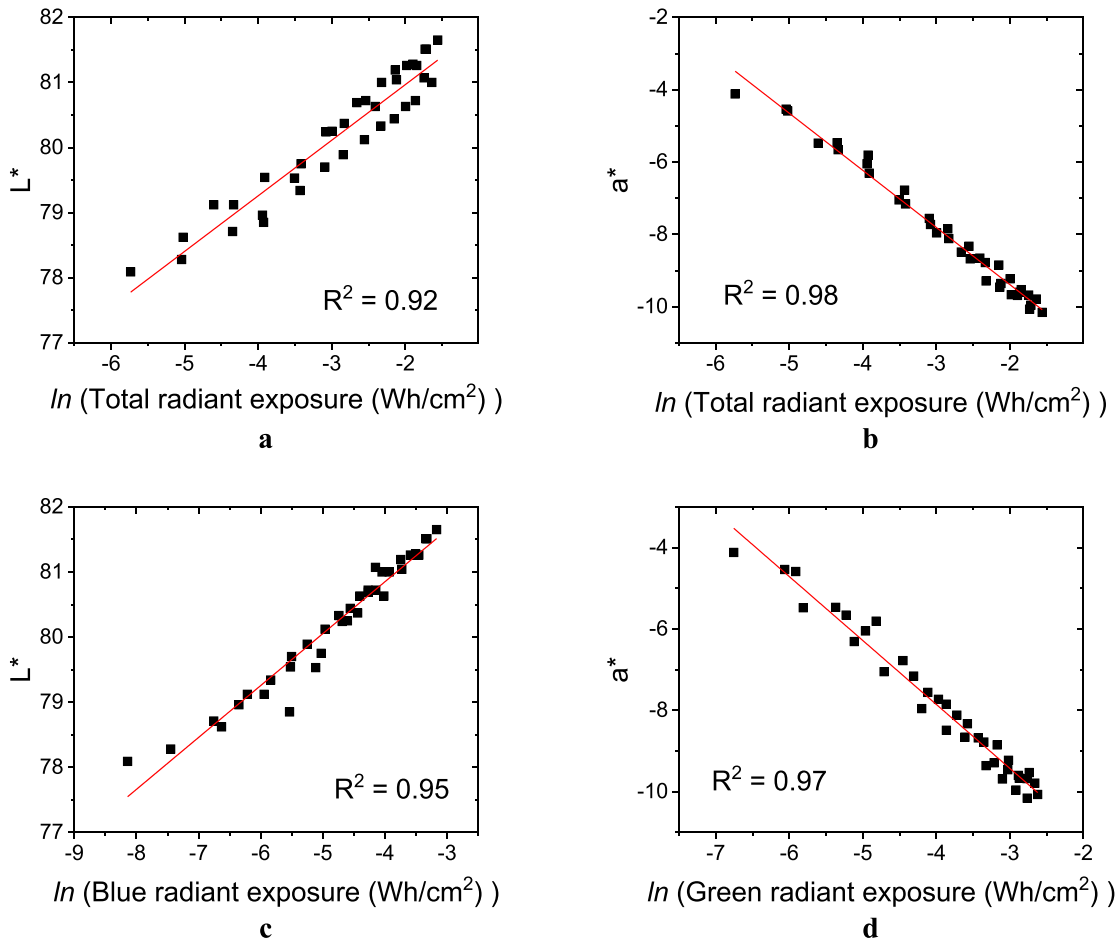

Figure 6. Plots of L^*, a^*, b^* values using the colour change model for strontium yellow oil paints.

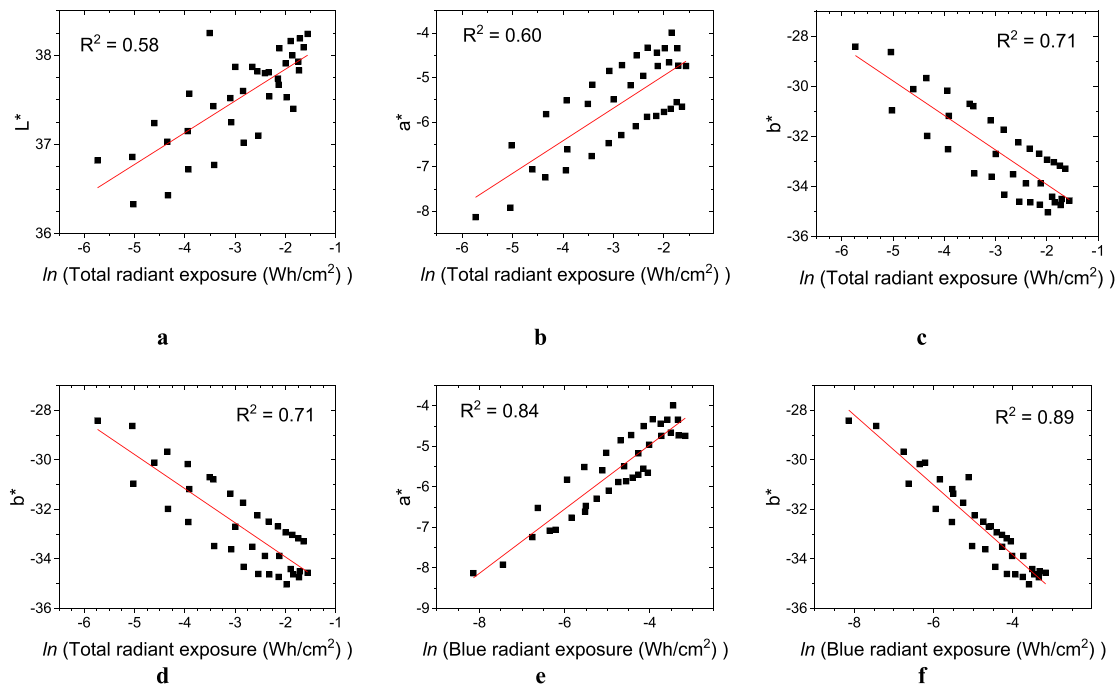

Figure 7. Plots of L^*, a^*, b^* values using the colour changing model for Prussian blue-lead white oil paints.

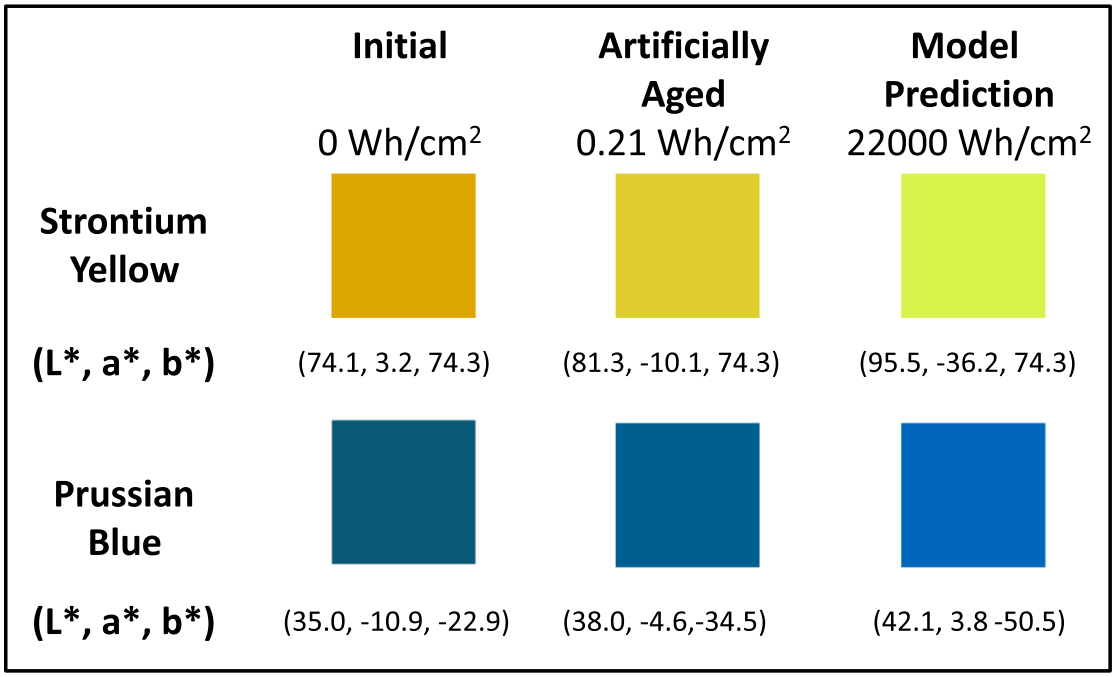

Figure 8. Initial colour, colour changes during artificial ageing and predicted colour change of strontium yellow and Prussian Blue-lead white pigments in the oil binder.

predicting or preventing long-term colour changes, making it an effective solution for conservation professionals and non-specialists alike.

However, we conducted a qualitative prediction to evaluate whether the methodology presented here can anticipate significant colour changes in historic paints. Figure 8 illustrates for the strontium yellow and Prussian blue-lead white oil paints, the initial colour, the colour changes observed after artificial ageing up to 0.21 Wh cm^{-2} of total radiant exposure, and the model predicted evolution of the colour change after 22 000 Wh cm^{-2} of total radiant exposure. Additionally, Prussian Blue-lead white paints become brighter and exhibit, that attributed this change to Fe(III)—> Fe(II) photoreduction, facilitated by the Fe(III)–CN ligand-to-metal charge transfer [30, 31, 42, 43]. These preliminary results provide an initial indication of the potential for colour change prediction using the proposed methodology.

4. Conclusions

This paper presents a new method to determine, model, and predict the potential shift, deterioration, or progressive loss of colour that can be caused by cumulative light exposure. The method is proposed as a tool for lighting design in museums or temporary exhibitions to help professionals design lighting to highlight objects while remaining within safe limits in terms of object protection/preservation. The method requires a minimum of technical information usually available from manufacturers, photometric measurements with simple and non-specialised equipment, and experimental artificial ageing data for pigments used for the modelling that can be continuously enriched by own measurements or by data available in repositories.

The discussed results on artificially aged paint samples—presented here as a case study—confirm that the rate of light-induced colour change depends on the light source, i.e. the spectral emission distribution of the source. This has already been documented in the literature and is specific to new technology (solid state) sources and therefore represents a new research need that we are called upon to address. The method considers the spectral profile of the light source without requiring a detailed measurement using a spectrophotometer. It is sufficient to measure the total irradiance on the object surface and to know the spectral profile (normalized curve) from which the percentage of the emission distribution in the three spectral regions R, G, B is calculated. These values allow a simple classification of the light sources based on their tri-spectral emission profile.

The introduced simple but highly effective model, combined with the simplified light source classification system, allows the evaluation and prediction of pigment colour changes under different lighting conditions, that is using different light sources in different lighting scenarios. The model was experimentally validated through artificial photo-ageing tests on oil paint mock-ups of two pigments with a long history of

use—strontium yellow and Prussian blue mixed with lead white (hydrocerussite)—using two WLEDs and a xenon light source. The results point out that the blue component (380–500 nm) of the emission is the primary driver of the lightness (L^*) changes in strontium yellow while the red component (600–780 nm) presents a slightly higher influence in the Prussian blue-lead white. The change in the a^* value of strontium yellow is independent of the spectral power distribution of the light source, while the b^* value did not show any significant change. For Prussian blue-lead white paints the a^* and b^* values show significant dependence on the blue spectral component.

Furthermore, plotting the L^*, a^* and b^* values against the natural logarithm of the radiant exposure showed a systematic linear relationship, confirming the accuracy and reliability of the proposed colour change model. This linearity allows the model to be used to predict long term pigment stability or susceptibility to colour change against cumulative light exposure over time.

Integrating the spectral classification of light sources with the colour change model provides more accurate insights into the causes of pigment degradation than traditional methods that rely solely on the total irradiance. This combined approach enables more reliable predictions of long-term colour changes, providing a valuable tool for conservation efforts. In addition, the simplicity and accessibility of the method constitutes a practical solution for both specialists and non-specialists enabling them to make informed decisions about the preservation of artworks. Future work could extend the applicability of the model by incorporating data for additional pigments and pigment-binder systems and a wider range of light sources, further enhancing its utility in diverse conservation contexts.

Although this study provides valuable insights, several limitations should be addressed in future work. The model proposed in this study assumes a direct correlation between colour changes (as indicated by shifts in L^*, a^*, and b^* values) and the decrease in original pigment concentration due to photochemical degradation; this assumption has limitations. Colour shifts can be due not only to the reduction of the original pigment concentration, but also to the formation of secondary degradation products, interactions with binders, or environmental factors that do not uniformly change concentration. Additionally, the degradation pathways of certain pigments are complex, and the photochemical reactions may not result in linear or directly predictable colour changes. Light exposure, environmental conditions such as temperature and UV radiation can significantly affect degradation pathways, particularly through oxidative reactions in drying oils or structural changes at the paint surface [44]. Incorporating these multi-stressor interactions would enhance the predictive realism of the model.

Therefore, extending the artificial ageing tests to a wider range of pigments with different chemical composition, (with priority given to) prioritising those that are highly sensitive to light and prone to alteration, such as chrome yellows, cadmium yellows, and cadmium reds, will strengthen the reliability and broader applicability of the model. In addition, the method will be expanded to include various light sources with different spectral power distributions. This combined development/expansion, increasing both number of pigments and light sources will enable a more comprehensive modelling of colour changes under diverse conditions.

Additionally, the data used in the model were obtained under constant atmospheric conditions, specifically stable temperature and relative humidity, as the current formulation of the model focuses on light exposure and does not account for environmental factors such as humidity, temperature, or pollutants. These variables can interact with light to accelerate pigment degradation, yet are excluded from the present model. Despite this limitation, the model remains highly applicable, particularly in museum settings where environmental conditions are generally controlled, especially when displaying fragile objects. Nevertheless, to enhance the model's real-world applicability across a broader range of conservation contexts, future research should integrate these environmental variables. The use of multi-factorial approaches, including machine learning, offers promising directions for developing more comprehensive predictions of pigment degradation under combined atmospheric and lighting conditions.

By addressing these limitations, future work can expand the model's utility, making it a more versatile and reliable tool for long-term preservation of historical artworks under a variety of environmental conditions.

Data availability statement

All data that support the findings of this study are included within the article (and any supplementary files).

Acknowledgment

We gratefully acknowledge the support for this study provided by the IPERION HS project (GA No. 871034) and the PERCEIVE project (GA No. 693529), both funded by the European Union's Horizon 2020 Research and Innovation Programme. The researchers of CNR-SCITEC also thank the Project PE 0000020 CHANGES

(Cultural Heritage Active Innovation for Next-Gen Sustainable Society)—CUP: B53C22003890006, NRP Mission 4 Component 2 Investment 1.3, funded by the EU—NextGenerationEU" under the Italian Ministry of University and Research (MUR), for supporting part of the research activities. The publication of the article in the Open Access journal was financially supported by HEAL-Link.

Author contributions

Panagiotis Siozos 0000-0002-4836-5557
Conceptualization (lead), Data curation (lead), Formal analysis (lead), Methodology (lead), Visualization (lead), Writing – original draft (lead), Writing – review & editing (lead)

Letizia Monico 0000-0001-9489-7805
Data curation (equal), Formal analysis (equal), Investigation (equal), Resources (equal), Validation (equal), Writing – original draft (equal), Writing – review & editing (equal)

Aldo Romani 0000-0002-7338-0097
Data curation (supporting), Resources (equal), Writing – original draft (supporting), Writing – review & editing (supporting)

Costanza Miliani 0000-0001-6091-9922
Project administration (supporting), Resources (equal), Supervision (supporting), Writing – review & editing (supporting)

Brenda Doherty 0000-0002-9326-2143
Resources (equal), Writing – review & editing (supporting)

Irina Crina Anca Sandu 0000-0002-3307-3682
Resources (equal), Writing – review & editing (supporting)

Hartmut Kutzke
Resources (supporting), Writing – review & editing (supporting)

Ingrid M T Flåte
Resources (supporting)

Petros Stavroulakis
Software (equal), Visualization (supporting), Writing – original draft (supporting), Writing – review & editing (supporting)

Sophia Sotiropoulou 0000-0001-9146-8474
Funding acquisition (lead), Methodology (equal), Project administration (equal), Supervision (lead), Visualization (supporting), Writing – original draft (equal), Writing – review & editing (equal)

References

[1] Anon 2022 *ICOM Standing Committee for the Museum Definition—ICOM Define Final Report (2020–2022)* (International Council of Museums)
[2] Welsh P H 2005 Reinventing the Museum: historical and contemporary perspectives on the paradigm shift *Mus. Anthropol.* **28** 67–72
[3] Sandell R and Nightingale E 2013 *Museums, Equality and Social Justice* (Routledge)
[4] Anon 2015 *Recommendation Concerning the Protection and Promotion of Museums and Collections Their Diversity and Their Role in Society Adopted by the General Conf. at Its 38th Session* (*Paris, 17 November 2015*)
[5] Saunders D 2020 *Museum Lighting: A Guide for Conservators and Curators* (The Getty Conservation Institute)
[6] Druzik J R and Michalski S W 2012 *Guidelines for Selecting Solid-State Lighting for Museums* (Getty Conservation Institute)
[7] Sanchez M 2013 Why online news reports claiming that LED exposure darkened the artist's colors were mistaken *Independent* (available at: www.independent.co.uk/arts-entertainment/art/news/sunflowers-wilt-van-gogh-s-masterpiece-is-slowly-turning-brown-as-a-result-of-exposure-to-led-lighting-8449304.html)
[8] Michalski S and Druzik J R 2020 *LED Lighting in Museums and Art Galleries* (Canadian Conservation Institute)
[9] Annis P A 2012 *Understanding and Improving the Durability of Textiles* (Woodhead publ)
[10] Zollinger H 2003 *Color Chemistry: Syntheses, Properties, and Applications of Organic Dyes and Pigments* (Verlag helvetica chimi acta Wiley-VCH)
[11] Anon Textiles—tests for colour fastness—part B02: colour fastness to artificial light: xenon arc fading lamp test ISO 105-B02:2014 (available at: https://www.iso.org/standard/65209.html)
[12] Aydemir C and Yenidoğan S 2018 Light fastness of printing inks: a review *J. Graph. Eng. Des.* **9** 37–43
[13] Wootton A 1992 Light fastness and weathering tests in the automotive industry *J. Soc. Dyers Colour* **108** 239–42
[14] Beltran V L, Druzik J and Maekawa S 2012 Large-scale assessment of light-induced color change in air and anoxic environments *Stud. Conserv.* **57** 42–57

[15] Farke M, Binetti M and Hahn O 2016 Light damage to selected organic materials in display cases: a study of different light sources *Stud. Conserv.* **61** 83–93
[16] Richardson E, Woolley E, Yurchenko A and Thickett D 2020 Assessing the impact of LED lighting on the stability of selected yellow paint formulations *LEUKOS* **16** 67–85
[17] Pintus V, Szabó F, Gazdag-Kéri R, Tóth D N, Nagy R, Csuti P, Sterflinger K and Schreiner M 2021 The effect of new LED lighting systems on the colour of modern paints *Sci. Rep.* **11** 22375
[18] Groeneveld I, Kanelli M, Ariese F and Van Bommel M R 2023 Parameters that affect the photodegradation of dyes and pigments in solution and on substrate—An overview *Dyes Pigm.* **210** 110999
[19] Lunz M, Talgorn E, Baken J, Wagemans W and Veldman D 2017 Can LEDs help with art conservation?—Impact of different light spectra on paint pigment degradation *Stud. Conserv.* **62** 294–303
[20] Monico L, Janssens K, Cotte M, Romani A, Sorace L, Grazia C, Brunetti B G and Miliani C 2015 Synchrotron-based x-ray spectromicroscopy and electron paramagnetic resonance spectroscopy to investigate the redox properties of lead chromate pigments under the effect of visible light *J. Anal. At. Spectrom.* **30** 1500–10
[21] Macchia A, Cesaro S N, Campanella L, Maras A, Rocchia M and Roscioli G 2013 Which light for cultural heritage: comparison of light sources with respect to realgar photodegradation *J. Appl. Spectrosc.* **80** 637–43
[22] Ford B and Smith N 2011 The development of a significance-based lighting framework at the National Museum of Australia *AICCM Bull.* **32** 80–86
[23] Dang R, Zhang F, Yang D, Guo W and Liu G 2020 Spectral damage model for lighting paper and silk in museum *J. Cult. Herit.* **45** 249–53
[24] International Commission on Illumination 2004 *Control of Damage to Museum Objects by Optical Radiation: Technical Report* (CIE)
[25] Garside D, Curran K, Korenberg C, MacDonald L, Teunissen K and Robson S 2017 How is museum lighting selected? An insight into current practice in UK museums *J. Inst. Conserv.* **40** 3–14
[26] Miliani C, Monico L, Melo M J, Fantacci S, Angelin E M, Romani A and Janssens K 2018 Photochemistry of artists' dyes and pigments: towards better understanding and prevention of colour change in works of art *Angew Chem., Int. Ed.* **57** 7324–34
[27] Otero V, Campos M F, Pinto J V, Vilarigues M, Carlyle L and Melo M J 2017 Barium, zinc and strontium yellows in late 19th–early 20th century oil paintings *Herit. Sci.* **5** 46
[28] Eastaugh N, Walsh V, Chaplin T and Siddall R 2008 *Pigment Compendium: A Dictionary and Optical Microscopy of Historical Pigments* (Butterworth-Heinemann)
[29] Ferrer J S, Sandu I C A, Syversen T, Cardoso A M, Candeias A and Borca C N 2019 Investigating colour changes in red and blue paints—a preliminary study of art materials and techniques in Edvard Munch's Old Man in Warnemünde (1907) *Conservation of Modern Oil Paintings* ed K J Van Den Berg, I Bonaduce, A Burnstock, B Ormsby, M Scharff, L Carlyle, G Heydenreich and K Keune (Springer International Publishing) pp 209–18
[30] Samain L, Grandjean F, Long G J, Martinetto P, Bordet P, Sanyova J and Strivay D 2013 Synthesis and fading of eighteenth-century Prussian blue pigments: a combined study by spectroscopic and diffractive techniques using laboratory and synchrotron radiation sources *J. Synchrotron Radiat.* **20** 460–73
[31] Samain L, Gilbert B, Grandjean F, Long G J and Strivay D 2013 Redox reactions in Prussian blue containing paint layers as a result of light exposure *J. Anal. At. Spectrom.* **28** 524
[32] Samain L *et al* 2011 Fading of modern Prussian blue pigments in linseed oil medium *J. Anal. At. Spectrom.* **26** 930
[33] Samain L, Grandjean F, Long G J, Martinetto P, Bordet P and Strivay D 2013 Relationship between the synthesis of prussian blue pigments, their color, physical properties, and their behavior in paint layers *J. Phys. Chem. C* **117** 9693–712
[34] Vila A, Monrad K, Filtenborg T and Wadum J 2020 As time passed by came sunset *Christen Købke's View of Lake Sortedam, Its Genesis and Colour Changes Science and Art* ed A Sgamellotti, B G Brunetti and C Miliani (Royal Society of Chemistry) Ch 17, pp 354–72
[35] Kirby J and Saunders D 2004 *Fading and Colour Change of Prussian Blue: Methods of Manufacture and the Influence of Extenders* Vol. 25 (National Gallery)
[36] Keune K 2023 *IPERION HS D.5.3 Protocol to Monitor Objects and Environment for Preventive Conservation and Concept of Digital Platform Infrastructure for Preventive Conservation (1.0)* (Zenodo) https://doi.org/10.5281/zenodo.10141823
[37] Hippler M 2003 Photochemical kinetics: reaction orders and analogies with molecular beam scattering and cavity ring-down experiments *J. Chem. Educ.* **80** 1074
[38] Michalski S 2020 CCI light damage calculator 1—single point source data (available at: https://herie.pl/Home/ManualLightDamageCalculator)
[39] Khalid S, Azad M M, Kim H S, Yoon Y, Lee H, Choi K-S and Yang Y 2024 A review on traditional and artificial intelligence-based preservation techniques for oil painting artworks *Gels* **10** 517
[40] Liu Z, Zhao A-R and Liu S-L 2024 Prediction of fading for painted cultural relics using the optimized gray wolf optimization-long short-term memory model *Appl. Sci.* **14** 9735
[41] Lerwill A, Brookes A, Townsend J H, Hackney S and Liang H 2015 Micro-fading spectrometry: investigating the wavelength specificity of fading *Appl. Phys. A* **118** 457–63
[42] Gervais C, Languille M-A, Réguer S, Gillet M, Pelletier S, Garnier C, Vicenzi E P and Bertrand L 2013 Why does Prussian blue fade? Understanding the role(s) of the substrate *J. Anal. At. Spectrom.* **28** 1600
[43] Gervais C, Languille M-A, Reguer S, Garnier C and Gillet M 2014 Light and anoxia fading of Prussian blue dyed textiles *Herit. Sci.* **2** 26
[44] Zuo S, Chen T, Li T, Li J and Liu X 2024 Degradation of oil paint coating based on wood under the combined effect of UV light and heat *Forests* **16** 22